Spectroscopic characterization and high antibacterial activity of silver nanoparticles functionalized Alpaca fibers

H. Félix-Quintero[a], S. R. Jáuregui-Rosas[b], F. V. Samanamud-Moreno[b], V. Montero-Del Aguila[b], G. G. Zavaleta-Espejo[c], J. A. Saldaña-Jiménez[c], E. V. Mejía-Uriarte[d], and C. M. Yee-Rendon[a]

[a]*Facultad de Ciencias Físico-Matemáticas, Universidad Autónoma de Sinaloa, Blvd. Universitarios S/N, 80020, Sinaloa, México.*
[b]*Laboratorio de Investigación en Nanociencia y Nanotecnología, Departamento de Física, Universidad Nacional de Trujillo, Av. Juan Pablo II S/N, Trujillo, Perú*
[c]*Laboratorio de Investigación en Bionanotecnología y Reproducción Animal, Departamento de Biología, Universidad Nacional de Trujillo, Av. Juan Pablo II S/N, Trujillo, Perú*
[d]*Instituto de Ciencias Aplicadas y Tecnología, Universidad Nacional Autónoma de México, Circuito Exterior S/N, Ciudad Universitaria, 04510, Ciudad de México, México.*

Received 17 July 2024; accepted 27 July 2025

Using a simple chemical solution synthesis method, silver nanoparticle-functionalized alpaca fibers were prepared. Special attention was paid to three natural colors of alpaca fibers: white, brown, and black, for the study of absorbance, excitation, emission, Raman, and FTIR spectra. The alpaca fibers at higher silver concentrations exhibited an efficient SERS effect on the melanin molecule, with two bands centered at 1568 and 1336 cm^{-1}. The first band originated from the in-plane stretching of the aromatic rings, and the latter from the linear stretching of the C=C bonds within the rings. This molecule increases antibacterial capacity by enhancing the presence of Ag+ ions. The fibers treated with silver showed excellent antibacterial activity against Escherichia coli ATCC 25922.

Keywords: Alpaca; E. coli; SERS effect; silver nanoparticle

DOI: https://doi.org/10.31349/RevMexFis.71.061602

1. Introduction

The development of multifunctional coatings on textiles is recognized as an attractive field due to its potential for practical applications. Researchers have been trying to introduce various characteristics to textiles, such as antimicrobial activity, antistatic capacity, self-cleaning properties, UV protection, thermoregulation, and electrical conductivity [1-4]. To achieve this, a broad range of materials, including nanoparticles (NPs) and thin films, have been used, with each functionality being achieved through different mechanisms and treatment protocols. Among the most studied functionalized textiles are wool, cotton, linen, silk, and more [5-7]. However, much less attention has been paid to Vicugna pacos (alpaca) fibers; in fact, studies on this type of animal fiber are practically non-existent. Alpaca fiber is similar in structure to sheep wool fiber [8], composed of the complex protein keratin and, in the case of colored fibers, melanin. The softness of alpaca fiber comes from its smoother scale surface compared to sheep wool. On the other hand, the Raman effect involves the inelastic scattering of light by molecules [9]. The scattered radiation contains information about vibrational states that is unique to any molecular system, and its intensity is directly proportional to the quantity of species involved in the process. However, Raman scattering is intrinsically weak, which significantly restricts the analysis of scattered molecular systems such as melanin in white fiber. This limitation has been overcome with the advent of Surface-Enhanced Raman Scattering (SERS) [10]. The SERS effect is an exceptional increase in Raman intensity observed for adsorbed molecules on surfaces. Typically, nanostructured surfaces of gold, silver, and copper are substrates with an efficient SERS response. The efficiency of the SERS signal strongly depends on the geometric characteristics of the metallic nanostructure, so tiny variations in molecular positions or the arrangement of metallic particles cause significant fluctuations in SERS intensity [11-13]. As a high chelating agent, melanin is known to capture and release metal ions without morphological changes [14,15], which could influence antibacterial activity by capturing Ag^{+} ions during the synthesis process. In this paper, the vibrational states of keratin and melanin in white, brown, and black silver-functionalized and non-functionalized alpaca fibers are studied using Raman spectroscopy, complemented by Fourier-transform infrared spectroscopy (FTIR). Raman studies show a significant SERS effect in melanin spectra due to the presence of Ag NPs in functionalized alpaca fibers. The presence of nano-sized Ag particles is confirmed by absorbance and reflectance spectroscopy, as well as by the color change in white alpaca fibers. The presence of Ag+ ions is demonstrated by excitation and emission spectroscopy of functionalized alpaca fibers, and their effect is tested through antibacterial properties.

2. Materials and methods

Silver nitrate with a purity of 99.8% and trisodium citrate (TSC) were purchased from Merck. The reagents were used without further treatment. White, brown, and black Alpaca Huacaya fibers were provided by the Universidad de Huancavelica. These fibers underwent ultrasonic cleaning in distilled water for 5 minutes and were then air-dried. The fibers were subsequently stored in a dry environment with silica gel. The silver functionalization of fibers was conducted using an in situ reduction method to deposit silver nanoparticles onto the fiber surfaces, aiming to assess the impact of varying TSC concentrations. For each fiber color, three independent experiments were performed with 100 mg samples to ensure consistency. The process began by heating 150 ml of distilled water to 95^o under vigorous stirring. Fibers were submerged for two minutes to promote uniform wetting, followed by the addition of 6 mg of silver nitrate to introduce silver ions. Two minutes later, TSC was added at concentrations of 2 mg (A), 6 mg (B), or 10 mg (C) to reduce the silver ions to metallic nanoparticles Ag° on the fibers. The mixture was stirred for 25 minutes at 95°C to facilitate nanoparticle formation and attachment. Post-reaction, the fibers underwent a 3-minute ultrasonic cleaning in distilled water to remove loosely bound particles and excess reagents, ensuring only firmly adhered nanoparticles remained. They were then air-dried and stored with silica gel to prevent moisture-induced degradation.

The increase in TSC concentration resulted in a gradual color change from yellow to dark yellow, indicating an increase in Ag NPs on the fiber surface. Simultaneously, similar solutions were prepared without fibers for Ag NPs solution absorbance analysis. Reflectance spectra of functionalized and non-functionalized fibers were obtained using a two-beam Lambda 750-Perkin Elmer spectrophotometer with a spectralon integration sphere. Ag NPs solution absorbance was collected with a Specord 600-Analitikjena UV-Vis spectrophotometer. Raman spectra were obtained with an Alpha 300R Witec system, equipped with a 532 nm laser. FTIR spectra were acquired using a Nicolet iS50-Thermo Scientific spectrometer in Attenuated Total Reflectance (ATR) mode. Excitation and emission spectra were obtained with a Perkin-Elmer LS55 fluorescence spectrometer. The antibacterial test was performed using Escherichia coli ATCC 25922, following the modified AATCC-100 standard test method to work with individual fibers. A bacterial suspension at a concentration of 1.5×10^8 CFU/mL in physiological saline solution was prepared. One milligram of white, brown, and black alpaca fibers at different concentrations was weighed. A series of test tubes were prepared with 1 mL of Muller Hinton broth plus the bacterial inoculum and 1 mg of fiber of each concentration and color, and incubated for 6 hours at 37 °C. The experiment was performed in triplicate. After incubation, the plate counting technique was applied, which involved taking an aliquot from each tube, making six dilutions, and seeding them to determine the percentage of reduction using the following equation: $R(\%) = ((Cf - Ci)/Cf) \times 100$, where R is the percentage reduction, Ci are the counted colonies of the bacteria without the fibers after six hours of incubation, and Cf are the counted colonies exposed to the functionalized fibers [16-18].

3. Results and discussion

Figure 1 shows the reflectance spectra of the non-functionalized alpaca fibers, as displayed in the inset. As can be clearly seen, the brown and black fibers exhibit a broad absorbance band that spans practically the entire visible spectrum. This band is attributed to the absorbance of the complex molecule melanin, which is present in colored fibers and appears to be absent in the white fibers, as expected [19].

Next, the Raman spectrum of the white fiber is shown in Fig. 2a), which displays the widely reported Raman characteristics of natural fibers [20]. All peaks correspond to the Raman spectrum of pure keratin, with the exception of the 3289 cm^{-1} band, which originates from OH molecules [21]. Figure 2b) shows the Raman spectra of the three non-functionalized fibers. The intensities have been adjusted to clearly display the differences between them. The main characteristic of the colored samples is the broad fluorescence band that spans the entire Raman spectrum and two relatively wide Raman absorption bands at 1568 and 1336 cm^{-1} in the black fiber.

These peaks are reported to be produced by the melanin molecule [14,15,19], with the first peak originating from the in-plane stretching of the aromatic rings and the latter from the linear stretching of the C=C bonds within the rings, with some contributions from the C-H vibrations in the methyl and methylene groups. The Raman spectrum of keratin and melanin in the brown fiber is not visible, likely due to the high absorbance around the 500 nm region, as seen in Fig. 1, which absorbs considerable laser power. It is unclear if the

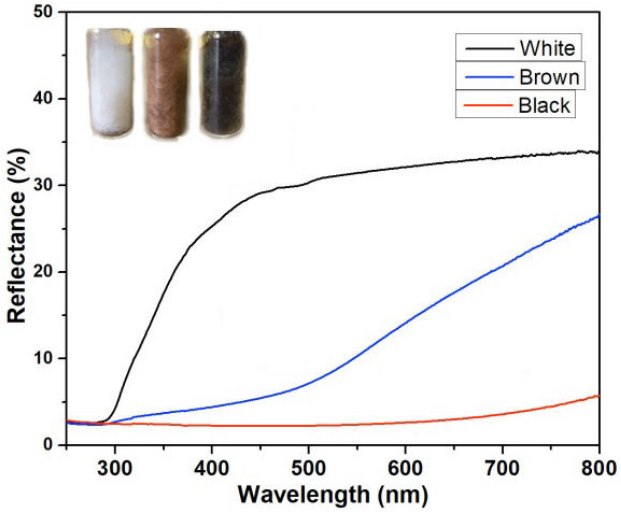

FIGURE 1. Reflectance spectra of white, brown, and black alpaca fibers as shown in the inset. The spectra highlight the high absorption capacity of the melanin molecule in the brown and black fibers.

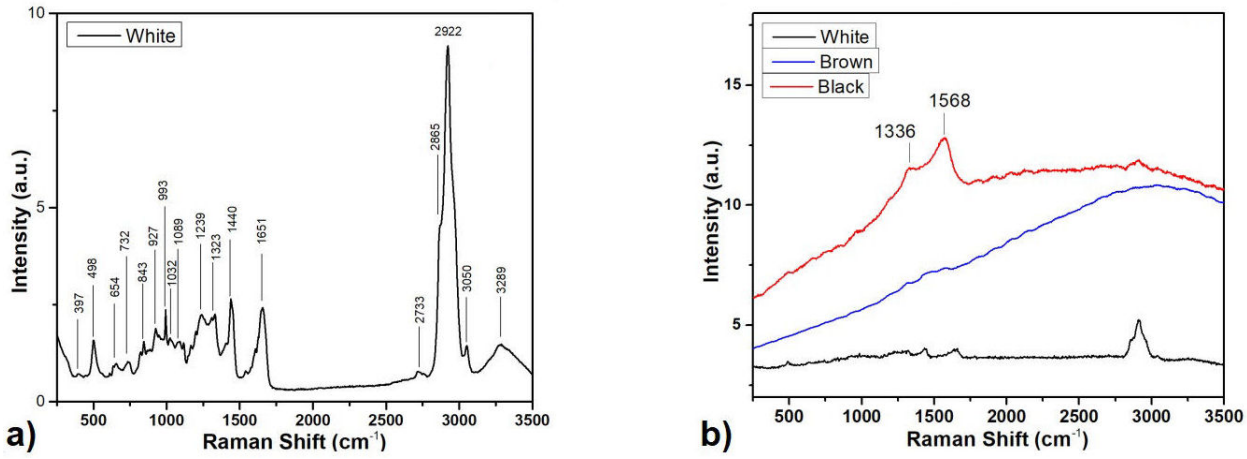

FIGURE 2. a) Raman spectrum of the white fiber, with all observed peaks labeled by their Raman shift values. b) Comparison of the Raman spectra of white, brown, and black alpaca fibers, clearly highlighting the melanin Raman spectrum in the black fiber.

TABLE I. Peak assignment of Keratin and Melanin Raman and FTIR spectra in white Alpaca fibers.

Raman Shift (cm^{-1})	FTIR absorbance	Band assigments	Raman Shift (cm^{-1})	FTIR absorbance	Band assigments
397		(NCC)Ala [20]		1388	Pyrrole ring stretching [23]
198		Disulfide Cys(S-S) strech[20]	1440	1448	CH2 bending mode [20]
654		Tyr [20]		1518-1568	C=C aromatic ring vibration/ Pyrrole ring stretching [23]
732		Trp [20]		1628	C=O stretching vibration [22,23]
843		Ring breathing mode of Tyr [20]	1651		C=O amide I [20]
927	928	Strerch C-C skeletal a-helix [20]	2733		CH stretching [20]
993		Symetric ring breathing of Phe [20]	2865	2845	CH stretching [20]
1032	1042	CH in-plane bending of Phe[20]	2922	2925	CH stretching [20]
	1077	ν(C-O) [23]		2961	CH stretching [20]
1089		CC skeletal, trans conformation, C-N stretch [20]	3050	3065	CH stretching [20]
1239	1232	Amide III (unordered) [23]	3289	3270	OH [20]
1323		CH2 bend, Trp [22]		3490	Amide A-NH stretching [20]

protrusions around 1500 cm^{-1} in the brown fiber are due to melanin or keratin because of the presence of the broad fluorescence band. An important point to note is that a significant amount of melanin molecules is required to obtain its Raman spectrum at acceptable intensity when using a 532 nm laser. However, we cannot conclude that all peaks observed in the Raman spectra of white alpaca fiber arise solely from keratin, nor can we assert that these fibers are completely devoid of melanin, as will be shown later in the FTIR spectra. Figure 3 shows the FTIR spectra for the three colors of the studied alpaca fibers. A high similarity with the Raman spectra of the white fiber can be observed. The differences between the Raman and FTIR spectra arise from the allowance of their vibrations, as can be quickly seen with the 1518 cm^{-1} peak, which is only FTIR active. This spectrum is very similar to that of pure melanin, with contributions from keratin [22], which agrees with the increase in absorbance intensity as melanin concentration increases from white to black fiber.

Table I can be constructed by following the work of various authors [20,22,23]. This table summarizes all Raman and FTIR peaks in the spectra by comparing them with the pure keratin and melanin Raman and FTIR spectra. It shows that melanin vibrations seem to be primarily IR active, while the keratin peaks are Raman active. The presence of melanin in the white fiber, as suggested by the FTIR spectra, can be confirmed by the SERS effect, as will be shown next.

The inset in Fig. 4a) shows a picture of non-functionalized and 2 mg TSC Ag-functionalized white alpaca fibers, where the color change from white to yellow is remarkable. This change is due to the surface plasmon resonance band (SPR) generated by the presence of silver nanoparticles. The figure shows their reflectance spectra,

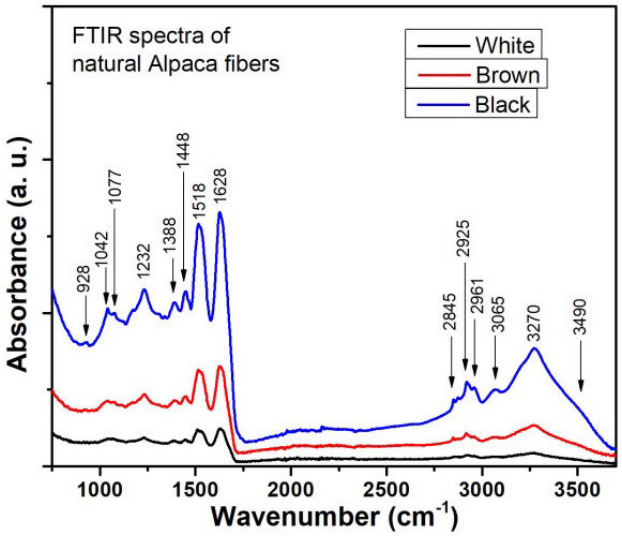

FIGURE 3. FTIR spectra of the three colors of non-functionalized Alpaca fibers.

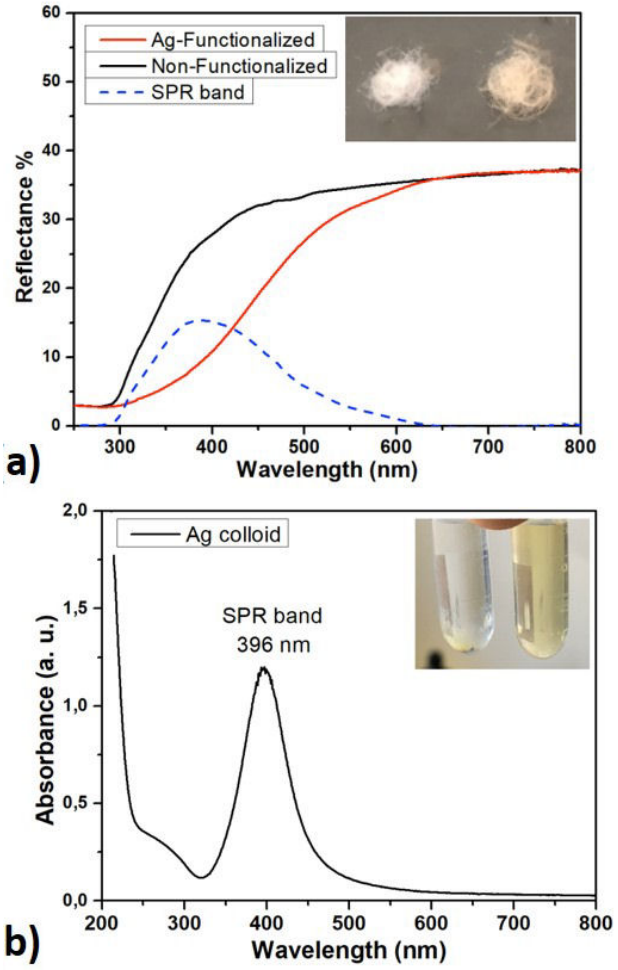

FIGURE 4. a) Reflectance spectra and their inverted subtraction to reveal the SPR band. The inset shows pictures of non-functionalized and Ag-functionalized white alpaca fibers. b) Absorbance spectrum of Ag NPs in colloidal form.

with an absorption band appearing around 400 nm in the Ag-functionalized fibers. The same figure shows, in blue dashed lines, the inverted subtraction of both non-functionalized and functionalized fibers reflectance, representing the SPR band. Similar SPR band characteristics can be confirmed in Ag NPs in colloidal form, as shown in Fig. 4b). The inset shows a picture of the solution with and without silver NPs. The position of the SPR band in the spectra confirms the presence of spherical Ag NPs with a mean diameter in the range of 10-20 nm [24].

Similar results cannot be observed in colored fibers due to their high intrinsic melanin absorbance around 400 nm. No noticeable color change is observed in Ag-functionalized brown and black fibers, as expected. The increase in TSC concentration during synthesis gradually shifts the coloration from yellow to dark yellow, indicating an increase in the quantity of Ag NPs on the fiber surface, which results in slight variations in the intensity of the reflectance spectra. As previously mentioned, Raman scattering is inherently weak, which significantly limits the analysis of dispersed molecular systems. Therefore, if melanin were present in the white fiber, it would be highly dispersed and at very low concentration. The melanin SERS effect can be detected, resulting in the SERS spectrum shown in Fig. 5a) for white fibers treated with 2, 6, and 10 mg of TSC. This clearly shows a melanin spectrum similar to that of black fiber, made possible only through the SERS effect. The intensity of melanin vibrations increases with higher TSC concentrations, indicating an increase in silver NPs on the fiber surfaces and thus an increase in the probability of SERS hot spots.

This spectrum confirms the presence of melanin in white alpaca fibers, as suggested by FTIR results, albeit at very low concentrations. When compared with the melanin spectrum of black fiber [Fig. 2b)], it is evident that the SERS effect yields a cleaner spectrum with less fluorescence. Similar results are observed in brown and black samples treated with 10 mg of TSC, as shown in Fig. 5b). The melanin spectrum is now more prominent compared to non-functionalized samples, with the SERS spot being easier to identify. No significant effect is observed in the FTIR spectra of silver-functionalized alpaca fibers. These results demonstrate that an important SERS effect can be achieved for detecting melanin in alpaca fibers, even in white fibers at very low concentrations, by using silver nanoparticles as a functionalizer.

The antibacterial efficacy of the silver-functionalized fibers was evaluated against E. coli. Figure 6 depicts the experimental setup. Figure 6a) displays the test tubes arranged from left to right: Muller Hinton broth, Muller Hinton broth with bacterial inoculum, and three replicates of Muller Hinton broth with bacterial inoculum and 1 mg of black fibers functionalized with 10 mg TSC. Figure 6b) illustrates the application of the plate counting technique, demonstrating the excellent antibacterial capability of the silver-functionalized fibers. Reduction in colony-forming units (CFU) was calculated, and the results are presented below. Table II summarizes the percentage reduction in the growth of Escherichia

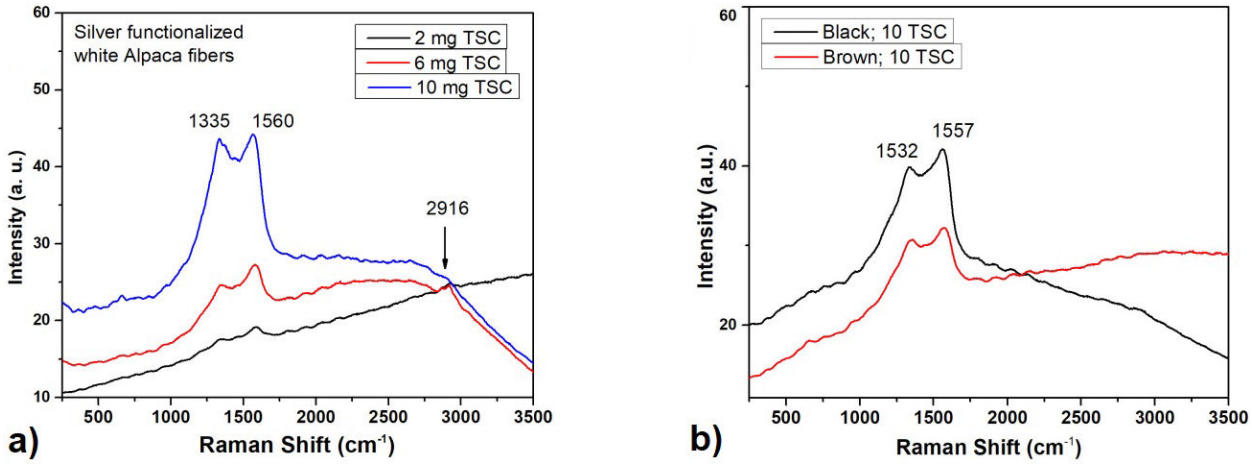

FIGURE 5. Raman spectra with SERS effect showing the melanin spectra on: (a) white and (b) brown and black Alpaca fibers.

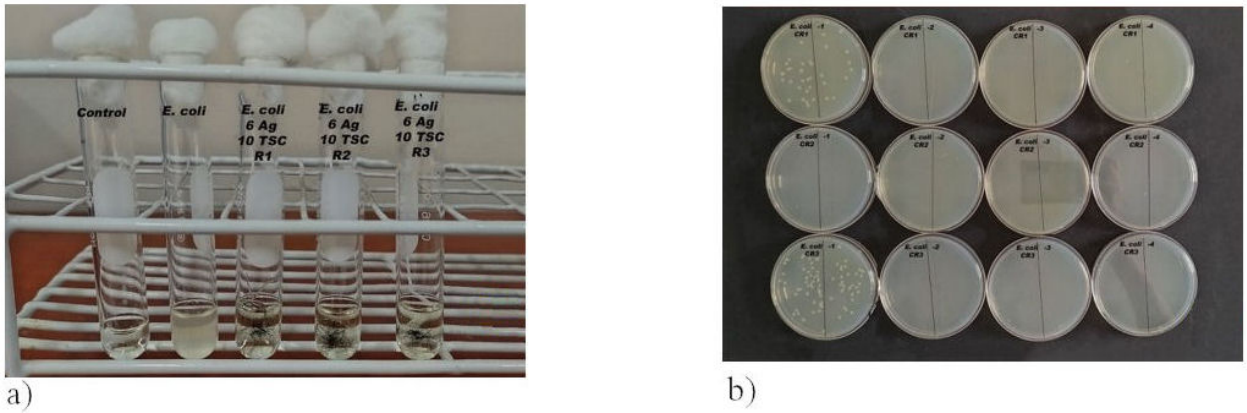

FIGURE 6. a) Test tubes arranged from left to right: Muller Hinton broth, Muller Hinton broth plus bacterial inoculum, and three replicates of Muller Hinton broth plus bacterial inoculum with 1 mg of black fibers functionalized with 10 mg TSC. b) Image demonstrating the plate counting technique.

TABLE II. Percentage reduction (%R) of *Escherichia coli* ATCC 25922 colony-forming units (CFU) after exposure to alpaca fibers functionalized with 6 mg of silver nitrate and varying concentrations of trisodium citrate (TSC): 0, 2, 6, and 10 mg. Fiber color, TSC concentration (mg), and CFU reduction (%) are shown.

Fiber Color	TSC concentration (mg)	Reduction of CFU(%)
White	2	93.58
	6	99.92
	10	99.80
Brown	2	99.60
	6	99.99
	10	99.99
Black	2	99.99
	6	99.99
	10	99.99

coli ATCC 25922 resulting from the bactericidal action of white, brown, and black alpaca fibers functionalized with silver at varying concentrations of trisodium citrate (TSC). Overall, the antimicrobial efficacy was comparable across all fiber colors, with only minor variations. Notably, the white fiber functionalized with the lowest concentration (6 mg of silver nitrate and 2 mg of TSC) exhibited a remarkably high bacterial reduction of 93.58% and no bacterial reduction was observed in the non-functionalized fibers. The antimicrobial mechanism of silver, particularly in its nanoparticle form, has been widely studied and documented in scientific literature [25-27]. Silver nanoparticles are known for their potent intrinsic bactericidal properties, which arise from their ability to release silver ions, disrupt bacterial cell membranes, generate reactive oxygen species (ROS), and interfere with essential microbial metabolic processes. Due to these well-established mechanisms, conducting additional antimicrobial tests on AgNPs alone is often considered redundant, as their effectiveness against a broad spectrum of bacteria, fungi, and even some viruses has been repeatedly confirmed.

However, the primary focus of this study lies not in reaffirming the inherent antibacterial activity of AgNPs but rather in their successful and stable immobilization onto Alpaca fibers, a key advancement that imparts significant antimicrobial functionality to the textile and the impact of melanin on

FIGURE 7. Antibacterial activity assay on *Escherichia coli* culture medium. The left sample corresponds to an unfunctionalized alpaca fiber, showing no inhibition of bacterial growth. The right sample shows a silver-functionalized alpaca fiber, evidenced by the clear inhibition zone surrounding the fiber. The background streaks indicate uniform bacterial growth across the medium.

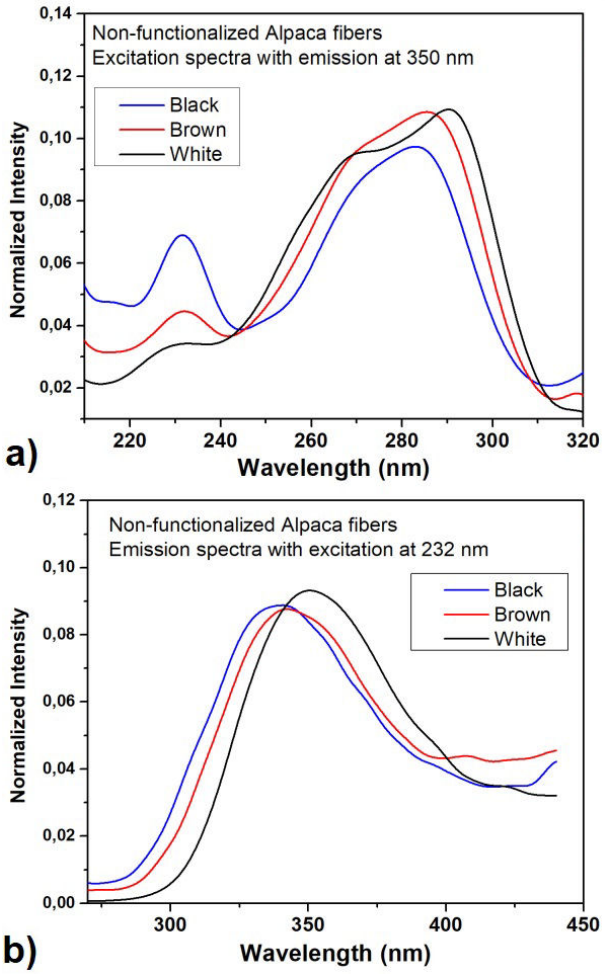

FIGURE 8. a) Excitation spectra of non-functionalized Alpaca fibers with emission at 350 nm. b)Emission spectra for the same samples with excitation at 232 nm.

on enhancing antibacterial properties. The reason for the increased reduction in these bacteria can be inferred by studying the emission and excitation spectra, which are presented next. Notably, untreated Alpaca fibers alone exhibit no inherent antimicrobial activity as seen in Fig. 7, as natural animal fibers typically lack inhibitory effects against microorganisms. This absence of antibacterial properties in the raw material underscores the critical role of AgNP immobilization in transforming the Alpaca fibers into an antimicrobial textile.

Figure 8a) shows the excitation spectra of the white, brown, and black non-functionalized Alpaca fibers with emission at 350 nm, while Fig. 8b) displays the corresponding emission spectra with excitation at 232 nm. The emission spectrum reveals a distinct ultraviolet band centered around 350 nm, which exhibits a blue shift as melanin concentration increases.The excitation spectra appear to consist of a 232 nm band and a relatively broad structured band centered at 280 nm.

The increased intensity of the 232 nm band as the fiber color transitions from white to black suggests its origin from melanin molecules, which are present in white fiber as previously demonstrated. It also appears that the 280 nm band is contributed to by both melanin and keratin molecules. The emission spectra observed upon excitation at 280 nm are very similar to those shown in Fig. 8b), with no additional emission peaks observed. The excitation spectrum for all silver-functionalized samples with emission at 350 nm is similar to that shown in Fig. 8a); however, the emission spectrum exhibits significant differences.

Figure 9a) displays the emission spectra with excitation at 232 nm for samples with higher TSC concentrations, where an additional blue band arises centered around 420 nm. The corresponding excitation spectrum for this band is shown in Fig. 9b). This blue emission and the energy levels observed in the excitation scheme correspond to the $4d^{10}(S) \rightarrow 4d^9 5s^1$(D) transition of Ag^+ ions [28]. The Russell-Saunders 1D and 3D states from the $4d^9 5s^1$ electronic configuration are split by spin-orbit coupling and ligand field effects. At the site of the Ag^+ ion, three transitions are allowed from the ground state to the excited levels, with peaks observed at 238 nm, 250 nm, and 268 nm, corresponding to the three allowed levels from the five excited states [$\Gamma M_\Gamma >$ from the 3D Russell-Saunders term of the C_4 symmetry, possible in the melanin complex structure [29]. The 420 nm emission observed in the 2 TSC and 6 TSC samples is similar to that shown in Fig. 7b) but with a slight increase in intensity in the 420 nm emission zone, so they were intentionally removed. The increase in blue emission with higher melanin concentration confirms its chelating effect, which enhances the presence of Ag^+ ions. The release of these ions, along with the slow release from Ag NPs, could contribute to the enhanced antibacterial effect; however, further detailed study is needed in future work to confirm this hypothesis. The apparent reduction of blue emission in black

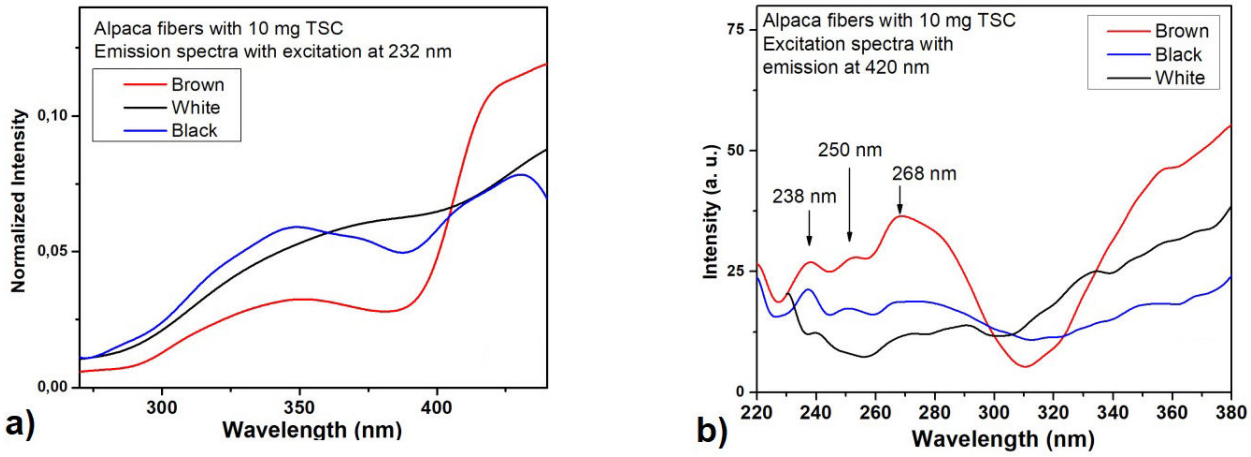

FIGURE 9. a) Emission spectra of 10 mg TSC silver-functionalized Alpaca fibers with excitation at 232 nm. b) Excitation spectra corresponding to an emission at 420 nm.

fibers may be attributed to melanin re-absorption of the emission, likely due to its higher concentration.

4. Conclusions

As demonstrated, the synthesis process used to produce silver-functionalized Alpaca fibers has proven highly effective in generating a strong SERS effect for detecting melanin, even in white fibers. High-quality Raman spectra of keratin molecules were also obtained, with all observed peaks in Raman and FTIR spectra for both keratin and melanin consistent with literature reports. This method could potentially be applied to other natural fibers with similar structures for the same purpose. Absorbance and reflectance spectra confirm the growth of spherical silver nanoparticles with mean diameters ranging from 10 to 20 nm using this synthesis process. Excitation and emission spectra indicate an increase in Ag+ ions with higher concentrations of melanin and TSC, highlighting the chelating effect of melanin. The functionality of TSC as a linker and reducing agent is confirmed, as reported by various authors. Furthermore, white, brown, and black Alpaca fibers functionalized with silver nanoparticles at varying concentrations of TSC exhibited excellent bactericidal activity against Escherichia coli ATCC 25922. Notably, black Alpaca fibers functionalized with silver nanoparticles and higher concentrations of TSC demonstrated superior bactericidal activity against Escherichia coli ATCC 25922.

Acknowledgments

The authors gratefully acknowledge the funding from Proyecto Concytec - Banco Mundial “Mejoramiento y Ampliación de los Servicios del Sistema Nacional de Ciencia Tecnología e Innovación Tecnológica” 8682-PE, supported by Fondecyt [Contract number 048-2019-FONDECYT-BM-INC.INV]. They also acknowledge financial support from the Consejo Nacional de Humanidades, Ciencias y Tecnología (Conahcyt) during the postdoctoral stay. Special thanks are extended to Dr. Gabriela Barraza (UNT) for providing facilities for FTIR measurements, and Dr. Paul Maihua (UNH) for assisting with fiber cleaning treatments.

1. E. Pakdel *et al.*, Advances in photocatalytic self-cleaning, superhydrophobic and electromagnetic interference shielding textile treatments, *Advances in Colloid and Interface Science* **277** (2020) 102116, https://doi.org/10.1016/j.cis.2020.102116
2. F. M. Kelly and J. H. Johnston, Colored and Functional Silver Nanoparticle-Wool Fiber Composites, *ACS Applied Materials & Interfaces* **3** (2011) 1083, https://doi.org/10.1021/am101224v
3. H. Y. Ki *et al.*, A study on multifunctional wool textiles treated with nano-sized silver, *Journal of Materials Science* **42** (2007) 8020, https://doi.org/10.1007/s10853-007-1572-3
4. S. Mowafi *et al.*, Facile and environmental benign in situ synthesis of silver nanoparticles for multifunctionalization of wool fibers, *Environmental Science and Pollution Research* **25** (2018) 29054, https://doi.org/10.1007/s11356-018-2928-8
5. H. Barani, M. N. Boroumand, and S. Rafiei, Application of silver nanoparticles as an antibacterial mordant in wool natural dyeing: *Synthesis, antibacterial activity, and color characteristics*, *Fibers and Polymers* **18** (2017) 658, https://doi.org/10.1007/s12221-017-6473-8
6. Y.-J. Tan *et al.*, A facile approach to fabricating silver-coated cotton fiber non-woven fabrics for ultrahigh electromagnetic interference shielding, *Applied Surface Science* **458** (2018) 236, https://doi.org/10.1016/j.apsusc.2018.07.107

7. A. Gao *et al.*, Efficient antimicrobial silk composites using synergistic effects of violacein and silver nanoparticles, *Materials Science and Engineering: C* **103** (2019) 109821, https://doi.org/10.1016/j.msec.2019.109821
8. C. Lupton, A. McColl, and R. Stobart, Fiber characteristics of the Huacaya Alpaca, *Small Ruminant Research* **64** (2006) 211, https://doi.org/10.1016/j.smallrumres.2005.04.023
9. R. Loudon, The Raman effect in crystals, *Advances in Physics* **13** (1964) 423, https://doi.org/10.1080/00018736400101051
10. M. Rycenga *et al.*, Understanding the SERS Effects of Single Silver Nanoparticles and Their Dimers, One at a Time, *The Journal of Physical Chemistry Letters* **1** (2010) 696, https://doi.org/10.1021/jz900286a
11. Y. Chen *et al.*, Self-assembly of Ag nanoparticles on the woven cotton fabrics as mechanical flexible substrates for surface enhanced Raman scattering, *Journal of Alloys and Compounds* **726** (2017) 484, https://doi.org/10.1016/j.jallcom.2017.07.315
12. D. Puchowicz *et al.*, Surface-enhanced Raman spectroscopy (SERS) in cotton fabrics analysis, *Talanta* **195** (2019) 516, https://doi.org/10.1016/j.talanta.2018.11.059
13. D. Cheng *et al.*, Depositing a flexible substrate of triangular silver nanoplates onto cotton fabrics for sensitive SERS detection, *Sensors and Actuators B: Chemical* **270** (2018) 508, https://doi.org/10.1016/j.snb.2018.05.075
14. W. L. Cheun, The Chemical Structure of Melanin, *Pigment Cell Research* **17** (2004) 422, https://doi.org/10.1111/j.1600-0749.2004.00165_1.x
15. Y. Liu *et al.*, Ion-Exchange and Adsorption of Fe(III) by Sepia Melanin, *Pigment Cell Research* **17** (2004) 262, https://doi.org/10.1111/j.1600-0749.2004.00140.x
16. M. E. El-Naggar *et al.*, Surface modification of SiO 2 coated ZnO nanoparticles for multifunctional cotton fabrics, *Journal of Colloid and Interface Science* **498** (2017) 413, https://doi.org/10.1016/j.jcis.2017.03.080
17. S. Dutta, T. Chowdhury, and A. Kumar Ghosh, Green synthesis of poly-L-lysine-coated sericin nanoparticles and their molecular size-dependent antibacterial activity, *Colloids and Surfaces B: Biointerfaces* **188** (2020) 110822, https://doi.org/10.1016/j.colsurfb.2020.110822
18. Z. Li *et al.*, The room temperature electron reduction for the preparation of silver nanoparticles on cotton with high antimicrobial activity, *Carbohydrate Polymers* **161** (2017) 270, https://doi.org/10.1016/j.carbpol.2017.01.020
19. Z. Huang *et al.*, Raman spectroscopy of in vivo cutaneous melanin, Journal of Biomedical Optics **9** (2004) 1198, https://doi.org/10.1117/1.1805553
20. M. Essendoubi *et al.*, Conformation changes in human hair keratin observed using confocal Raman spectroscopy after active ingredient application, *International Journal of Cosmetic Science* **41** (2019) 203, https://doi.org/10.1111/ics.12528
21. B. M. Auer and J. L. Skinner, IR and Raman spectra of liquid water: Theory and interpretation, *The Journal of Chemical Physics* **128** (2008), https://doi.org/10.1063/1.2925258
22. S. Sun *et al.*, Production of natural melanin by Auricularia auricula and study on its molecular structure, Food Chemistry **190** (2016) 801, https://doi.org/10.1016/j.foodchem.2015.06.042
23. S. Balaji *et al.*, Preparation and comparative characterization of keratin-chitosan and keratin-gelatin composite scaffolds for tissue engineering applications, *Materials Science and Engineering: C* **32** (2012) 975, https://doi.org/10.1016/j.msec.2012.02.023
24. D. Paramelle *et al.*, A rapid method to estimate the concentration of citrate capped silver nanoparticles from UV-visible light spectra, *The Analyst* **139** (2014) 4855, https://doi.org/10.1039/c4an00978a
25. I. Sondi and B. Salopek-Sondi, Silver nanoparticles as antimicrobial agent: a case study on E. coli as a model for Gram-negative bacteria, *Journal of Colloid and Interface Science* **275** (2004) 177, https://doi.org/10.1016/j.jcis.2004.02.012
26. W.-R. Li *et al.*, Antibacterial activity and mechanism of silver nanoparticles on Escherichia coli, *Applied Microbiology and Biotechnology* **85** (2009) 1115, https://doi.org/10.1007/s00253-009-2159-5
27. C.-N. Lok *et al.*, Silver nanoparticles: partial oxidation and antibacterial activities, *JBIC Journal of Biological Inorganic Chemistry* **12** (2007) 527, https://doi.org/10.1007/s00775-007-0208-z
28. H. Félix-Quintero *et al.*, Tunable white light emission through energy transfer processes between silver species in Ag-doped zinc phosphate glass, *Journal of Luminescence* **222** (2020) 117122, https://doi.org/10.1016/j.jlumin.2020.117122
29. S. Meng and E. Kaxiras, Theoretical Models of Eumelanin Protomolecules and their Optical Properties, *Biophysical Journal* **94** (2008) 2095, https://doi.org/10.1529/biophysj.107.121087